



ECMI Modelling Week, July 17–24, 2016, Sofia, Bulgaria

Group 4

Drug delivery from polymeric contact lenses

Amadou Yoro Thiam

University of Joseph Fourier, Grenoble, France
amadouyorotheiam@yahoo.fr

Billy Braithwaite

University of Jyväskylä, Finland
billy.h.v.braithwaite@jyu.fi

Emmy Sjöstrand

Lund University, Sweden
emmysjostrand@gmail.com

Javier García Bautista

University of Santiago de Compostela, Spain
javiertronco@hotmail.com

John McGowan

University of Strathclyde, Scotland
john.mcgowan@strath.ac.uk

Instructor: José Augusto Ferreira

University of Coimbra, Portugal
ferreira@mat.uc.pt

Contents

4.1	Introduction	1
4.2	Diffusion problem	1
4.2.1	Modelling	2
4.2.2	Computational domain and boundary conditions	4
4.2.3	Finite element method (FEM) formulation	4
4.3	Fluid dynamics problem	5
4.3.1	Modelling	5
4.3.2	Computational domain and boundary conditions	7
4.3.3	Finite element method (FEM) formulation	7
4.4	Numerical results and analysis	9
4.4.1	Meshing	9
4.4.2	Pressure field	10
4.4.3	Velocity field	10
4.4.4	Concentration field	10
4.5	Conclusions and outlook	11
	Bibliography	13

Abstract. Diseases of the anterior segment of the eye are mostly treated by topical administration in the anterior fornix of the conjunctiva. Nevertheless the procedure is extremely inefficient because when a drop is instilled in the eye, the ophthalmic drug has a short residence time in the conjunctiva sac, less than 5 minutes. Moreover, only 1–5% of the applied drug penetrates in the cornea reaching the intraocular tissue. To avoid the drawbacks of the topical administration, therapeutic lenses were designed to increase the ocular bioavailability of the ophthalmic drugs. A polymer is combined with drug in a such a way that the release profile is predefined. Several types of lenses were proposed: simple polymer membranes with dispersed drug, polymeric platforms with dispersed particles encapsulating drug and multilayer lenses. The main objective of this work is to study the drug evolution in the anterior chamber when different polymeric platforms are used to deliver the drug.

4.1 Introduction

The eye is a very complex organ. To take a simple structure of eye, we distinguish the anterior chamber, cornea and lens. There is a movement of fluid in the anterior chamber, this liquid is called aqueous humor and his quantity determine the intraocular pressure - IOP.

Sometimes we assist to the increasing of IOP (greater than 21mmHg). It could be due to inflammation of the trabecular mesh or an abnormal production of aqueous liquid. And this increasing of pressure damage the optic nerves. It is called Glaucoma.

Actually there exist several treatments such as once using therapeutical lenses. The problem with drugs is that with the large amount of aqueous humor in the anterior chamber, only a very small portion of the particles reach the conjunctiva. So it is not very effective. There is also the laser option but it is not a sustainable solution. We are especially interested in the therapeutic lens. This is to increase the effectiveness of the particles and the particle resistance time.

Our main goal is to look to see how the concentration in the anterior chamber changes over time. So we will make simulations on the trabecular wicks.

We organised our work into two parts. There are the Diffusion problem and Fluid dynamics problem. In Section 4.2 we present the Diffusion problem, and the Fluid dynamics notion is derived in the section 4.3. Then some numerical experiments are presented in Section 4.4.

4.2 Diffusion problem

If in a material there happens to be a difference in concentration of a chemical species over some distance, then in general, the differences tend to even out over time. The state at which the material no longer has any spatial concentration gradients is called an equilibrium. The physical process of diffusion is what drives a chemical species to achieve this equilibrium, causing the movement of

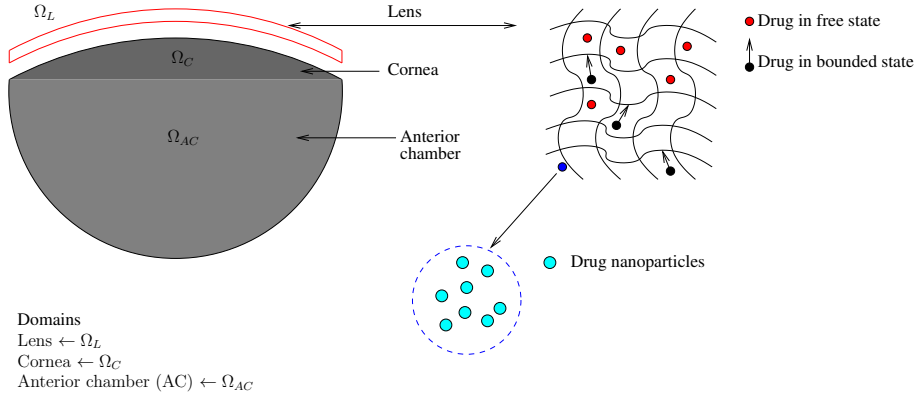


Figure 4.1: Drugs in the lens

the molecules from regions of high concentration to regions of low concentration. Diffusion is produced by the vibrations of atoms due to their thermal energy, making the atoms move on a random walk. The vibrations lead to atoms, that are spatially local enough, interacting and transferring energy between each other, which results in a net movement of molecules. Looking at the effects of these individual interactions on a fluid at a macroscopic scale, we see the fluid gradually spreading out far enough so that these local interactions between atoms or molecules is minimised at every point in the fluid. This is when the equilibrium state is achieved.

In the case of the anterior region of the eye, diffusion occurs in the polymeric contact lens, cornea and anterior chamber, denoted by Ω_L , Ω_C and Ω_{AC} , respectively. We allow the drug to take three different forms, namely; free drug, bound drug and entrapped drug. Free drug is contained within the threads of the polymer and is able to move ‘freely’ within this structure. This is the only drug form which can diffuse from the lens into the cornea. The bound drug is attached to the polymer threads, but this is not a fixed phenomenon. We allow for there to be chemical reactions which lead to binding of free drug to the polymer, and unbinding of the bound drug to become free drug. Finally, there can be drug particles entrapped within nanoparticles that gradually release free drug into the polymer.

Fig. 4.1 shows the three regions under consideration alongside the polymer containing the different drug forms.

4.2.1 Modelling

The mathematical model for the diffusion problem in the lens is a system of three coupled ODEs:

$$\frac{\partial C_f}{\partial t} = \nabla \cdot (D_l \nabla C_f) + \lambda_1(C_b - C_f) + \lambda_2(C_e - C_f)$$

$$\frac{\partial C_b}{\partial t} = -\lambda_1(C_b - C_f)$$

$$\frac{\partial C_e}{\partial t} = -\lambda_2(C_e - C_f)$$

where

- C_f : – Concentration of free drug
- C_b : – Concentration of bound drug
- C_e : – Concentration of entrapped drug
- D_l : – Diffusion coefficient in the lens
- λ_1 : – rate of binding/unbinding between drug and polymeric lens
- λ_2 : – rate of release of entrapped drug from nanoparticles

This system holds in the domain of the lens over a certain length of time, $\Omega_l \times (0, T]$

The only process in the cornea is diffusion and so the model is simply

$$\frac{\partial C_c}{\partial t} = \nabla \cdot (D_c \nabla C_c)$$

where

- C_c : – Concentration of drug in cornea
- D_c : – Diffusion coefficient in the cornea

The final region that the drug can make its way into by diffusion is the anterior chamber. Here we have the process of advection as well as diffusion, so the model is an advection-diffusion equation:

$$\frac{\partial C_{ac}}{\partial t} = \nabla \cdot (D_{ac} \nabla C_{ac}) - \mathbf{v} \nabla C_{ac}$$

where

- C_{ac} : – Concentration of drug in anterior chamber
- D_{ac} : – Diffusion coefficient in the anterior chamber

For the sake of simulations, we decided to largely simplify the model so that only diffusion can occur in the lens. In this case the full system reduces to:

$$\frac{\partial C_l}{\partial t} = \nabla \cdot (D_l \nabla C_l)$$

$$\frac{\partial C_c}{\partial t} = \nabla \cdot (D_c \nabla C_c)$$

$$\frac{\partial C_{ac}}{\partial t} = \nabla \cdot (D_{ac} \nabla C_{ac}) - \mathbf{v} \nabla C_{ac}$$

Initial conditions:

$$C(x, 0) = \begin{cases} C_l(x, 0) = C_0, & x \in \Omega_l \\ C_c(x, 0) = 0, & x \in \Omega_c \\ C_{ac}(x, 0) = 0, & x \in \Omega_{ac} \end{cases}$$

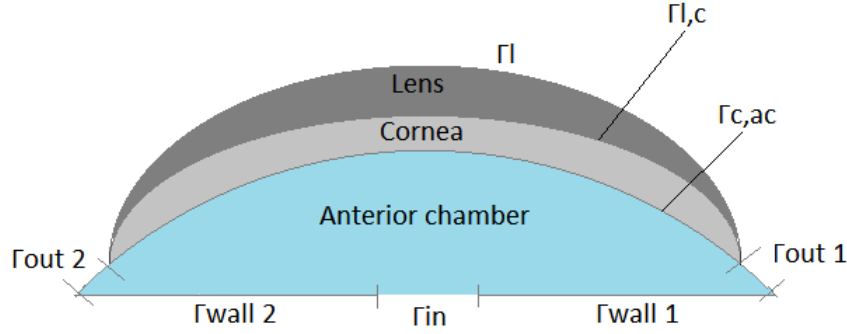


Figure 4.2: Simplified geometry. The shape is based on [1].

4.2.2 Computational domain and boundary conditions

The domain and boundary curves are displayed in Fig. 4.2.

The symbol \mathbf{J} denotes the mass flux of the drug. In the interest of continuity, the mass fluxes must be equal at the boundary curves between regions.

Boundary conditions for the drug in the lens:

- $\mathbf{J}_l(x, t) \cdot \boldsymbol{\eta}_l = 0, \quad x \in \Gamma_l, \quad t \in (0, T]$
- $\mathbf{J}_c(x, t) \cdot \boldsymbol{\eta}_c + \mathbf{J}_l(x, t) \cdot (-\boldsymbol{\eta}_c) = 0, \quad x \in \Gamma_{l,c}, \quad t \in (0, T]$

Boundary conditions for the drug in the cornea:

- $\mathbf{J}_c(x, t) \cdot \boldsymbol{\eta}_c + \mathbf{J}_l(x, t) \cdot (-\boldsymbol{\eta}_c) = 0$ on $\Gamma_{l,c}$
- $\mathbf{J}_{ac}(x, t) \cdot \boldsymbol{\eta}_{ac} + \mathbf{J}_c(x, t) \cdot (-\boldsymbol{\eta}_{ac}) = 0$ on $\Gamma_{c,ac}$
- $\mathbf{J}_{ac}(x, t) \cdot \boldsymbol{\eta}_{ac} + \mathbf{J}_c(x, t) \cdot (-\boldsymbol{\eta}_{ac}) = 0$ on $\Gamma_{c,ac}$

Boundary conditions for the fluid velocity in the anterior chamber:

$$\mathbf{v} = \begin{cases} \hat{v}_{in}, & x \in \Gamma_{in} \\ \hat{v}_{out1}, & x \in \Gamma_{out1} \\ \hat{v}_{out2}, & x \in \Gamma_{out2} \\ 0, & x \in \Gamma_{wall1} \cup \Gamma_{wall2} \cup \Gamma_{c,ac} \end{cases}$$

4.2.3 Finite element method (FEM) formulation

The variational formulation of the diffusion problem, with $\mathbf{v} = (v_1, v_2) \in H_0^1(\Omega) \times H_0^1(\Omega)$ and $\phi \in H_0^1(\Omega)$, is as follows:

$$\left(\frac{\partial C}{\partial t}, \phi \right) + (\nabla(C\mathbf{v}), \phi) = (\nabla(D\nabla C), \phi) + (R(C), \phi)$$

where:

$$\begin{aligned} (\nabla(C\mathbf{v}), \phi) &= \int_{\Omega} \nabla \cdot (C\mathbf{v})\phi \, dx = \int_{\partial\Omega} C\mathbf{v}\phi \cdot \boldsymbol{\eta} \, dS - \int_{\Omega} C\mathbf{v} \cdot \nabla\phi \, dx \\ (\nabla \cdot (D\nabla C), \phi) &= - \int_{\Omega} D\nabla C \cdot \nabla\phi \, dx \end{aligned}$$

Then, finally the weak problem is formulated as:

Find $\phi \in H_0^1(\Omega)$ such that:

$$\left(\frac{\partial C}{\partial t}, \phi \right) - (C\mathbf{v}, \nabla\phi) = (D\nabla C, \nabla\phi) + (R(C), \phi)$$

$$\forall \mathbf{v} = (v_1, v_2) \in H_0^1(\Omega) \times H_0^1(\Omega).$$

Discretization

For $C_h(t) \in V_{h,1}$ and $\forall \phi_h \in V_{h,1}$,

$$\left(\frac{\partial C}{\partial t}, \phi_h \right) - (C\mathbf{v}, \nabla\phi_h) - (D\nabla C, \nabla\phi) = (-\alpha C_h(t), \phi)$$

$$\begin{cases} \left(\frac{C_h^{n+1} - C_h^n}{\Delta t}, \phi_h \right) + (D\nabla C_h^{n+1}, \nabla\phi_h) - (v_h C_h^{n+1}, \nabla\phi_h) = -(\alpha C_h^n, \phi_h) \\ C_h^{(0)} = \tilde{C}_h, \quad i = 0, \dots, N \end{cases}$$

4.3 Fluid dynamics problem

The anterior segment of eye is filled with a transparent fluid, called *aqueous humor*. Anterior segment of the eye is comprised of two chambers, the anterior chamber (between the iris and the cornea) and posterior chamber (the region behind the iris and the anterior to the lens). The aqueous humor is secreted continuously by the ciliary epithelium in to the posterior chamber of the eye. It flows through the pupil aperture in the centre of the back wall of the anterior chamber, in order to reach anterior chamber. Aqueous humor occupying the anterior chamber provides a transparent medium for its optical function and regulates the intraocular pressure. Besides, it forms part of the pathway for topically applied drugs and for nutritional supply to and metabolites removal from avascular cornea [4]. Aqueous humour leaves the anterior chamber through the porous trabecular meshwork and flows into the Schlemm's canal. Outflow of aqueous humor regulates the intraocular pressure (IOP). The process is shown in Fig. 4.3.

4.3.1 Modelling

The non-dimensional analysis of the fluid dynamics problem is reduced to the study of the Reynolds number because the fluid problem is treated as dynamic. Following that idea, the viscosity and density of the aqueous humor are treated

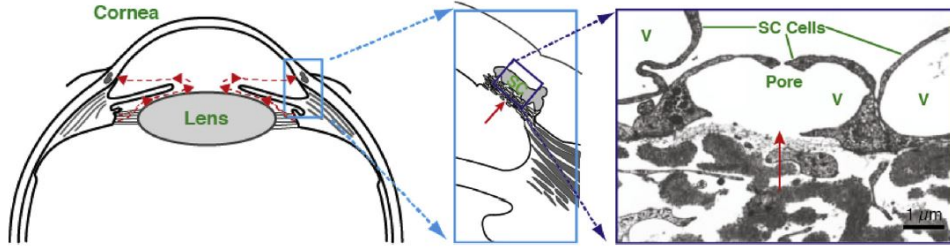


Figure 4.3: Aqueous humor flow pathway [3].

as the same as water and constant through the problem. Those two intensive properties are considered under standard conditions for temperature and pressure of 20 °C and 1 atm. Consequently¹:

$$Re = \frac{LU}{\nu} \approx 0,1 \sim 1$$

where:

L = anterior chamber height (characteristic length $\approx 0,3$ mm)

U = input flow velocity (max velocity ranges from 0,2 – 0,3 mm s⁻¹)

ν = kinematic viscosity of water ($\approx 0,7$ mm² s⁻¹)

It is assumed that the flow of the aqueous humor inside the anterior chamber is bidimensional and steady. Additionally, the flow is incompressible and laminar ($Re \approx 0,1$). Hence, under subsonic velocities, as the range of velocities described in the problem, $M \ll 1$, the continuity and momentum equation are decoupled from the energy equation and can be solved separately. Furthermore, because it is dynamic problem the energy equation is not required to be solved. Lastly, the fluid used is a Newtonian fluid and the gravitational forces are neglected. Therefore, the Navier-Stokes equations are described as:

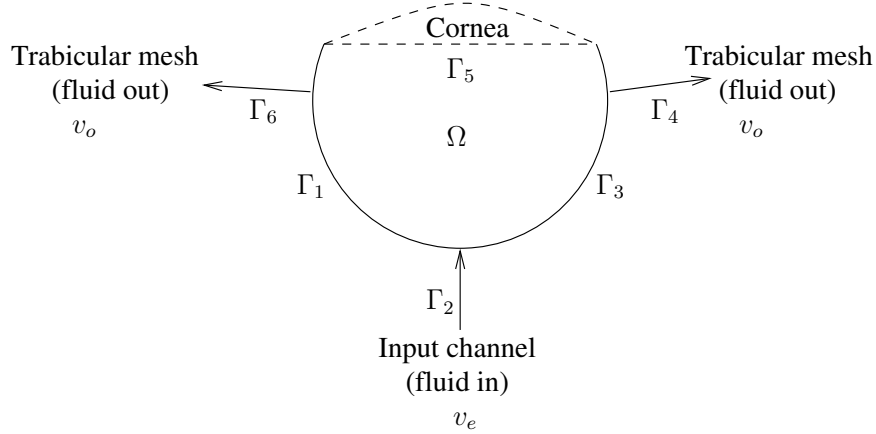
$$\nabla \cdot \mathbf{v} = 0$$

$$(\mathbf{v} \cdot \nabla)\mathbf{v} - \nu \Delta \mathbf{v} = -\nabla p$$

where \mathbf{v} is the velocity of the fluid (mm s⁻¹), p its specific pressure (kPa mm³ kg⁻¹), and ν its cinematic viscosity (mm² s⁻¹). In bidimensional form, $\mathbf{v} = (v_1, v_2)$, and the Navier-Stokes equations can be expressed as:

$$\begin{aligned} \left(\frac{\partial v_1}{\partial x} + \frac{\partial v_2}{\partial y} \right) &= 0 \\ \left(v_1 \frac{\partial v_1}{\partial x} + v_2 \frac{\partial v_1}{\partial y} \right) - \nu \left(\frac{\partial^2 v_1}{\partial x^2} + \frac{\partial^2 v_1}{\partial y^2} \right) &= -\frac{\partial p}{\partial x} \\ \left(v_1 \frac{\partial v_2}{\partial x} + v_2 \frac{\partial v_2}{\partial y} \right) - \nu \left(\frac{\partial^2 v_2}{\partial x^2} + \frac{\partial^2 v_2}{\partial y^2} \right) &= -\frac{\partial p}{\partial y} \end{aligned}$$

¹the units are in IS standard, except that *millimetres* is used instead of *metres*, due to the reduced dimensions of the problem



Ω := Anterior chamber (domain)
 $v = \hat{v}_2$ on Γ_2
 $v = \hat{v}_4$ on Γ_4
 $v = \hat{v}_6$ on Γ_6
 $v = 0$ on $\Gamma \setminus \Gamma_{2,4,6}$
 $v_i = \text{known}$ for $i = 2, 4, 6$

Figure 4.4: Fluid boundary conditions with simplified geometry.

4.3.2 Computational domain and boundary conditions

A dynamic flow is supposed to occur between the ciliary epithelium and the Schlemm's canal. However, to simplify the model, only the anterior chamber domain is modelled. Therefore, the aqueous humor enters the anterior chamber at the bottom part of the domain (input, Γ_2), flows through the chamber towards the lateral sides, and finally it flows into Schlemm's canals (outputs, Γ_6, Γ_4), that remove the liquid from the anterior chamber. The rest of the boundary (bottom, lateral and upper sides) behave as a wall (non-slip condition, $\Gamma_1, \Gamma_3, \Gamma_5$). The domain is both shown in Fig. 4.2 (together with cornea and contact lens domains) and Fig. 4.4 (exclusively the fluid domain).

4.3.3 Finite element method (FEM) formulation

The variational formulation of the Navier-Stokes equations, with $\mathbf{v} = (v_1, v_2) \in H_0^1(\Omega) \times H_0^1(\Omega)$, $\mathbf{u} = (u_1, u_2) \in H_0^1(\Omega) \times H_0^1(\Omega)$ and $p, q \in L^2(\Omega)$, is presented as follows:

$$\begin{cases} ((\mathbf{v} \cdot \nabla) \mathbf{v}, \mathbf{u}) - \nu(\Delta \mathbf{v}, \mathbf{u}) = -(\nabla p, \mathbf{u}) \\ (\nabla \cdot \mathbf{v}, q) = 0 \end{cases}$$

where:

$$\begin{aligned}
(\Delta \mathbf{v}, \mathbf{u}) &= (\Delta v_1, u_1) + (\Delta v_2, u_2) \\
&= \int_{\partial\Omega} \nabla v_1 \cdot \boldsymbol{\eta} u_1 \, dS - \int_{\Omega} \nabla v_1 \cdot \nabla u_1 \, d\Omega + \int_{\partial\Omega} \nabla v_2 \cdot \boldsymbol{\eta} u_2 \, dS - \int_{\Omega} \nabla v_2 \cdot \nabla u_2 \, d\Omega \\
&= - \int_{\Omega} \nabla v_1 \cdot \nabla u_1 \, d\Omega - \int_{\Omega} \nabla v_2 \cdot \nabla u_2 \, d\Omega \\
(\nabla p, \mathbf{u}) &= \int_{\Omega} \left(\frac{\partial p}{\partial x} u_1 + \frac{\partial p}{\partial y} u_2 \right) \, d\Omega \\
&= \int_{\partial\Omega} p \mathbf{u} \cdot \boldsymbol{\eta} \, dS - \int_{\Omega} \left(p \frac{\partial u_1}{\partial x} + p \frac{\partial u_2}{\partial y} \right) \, d\Omega \\
&= - \int_{\Omega} p \cdot \mathbf{u} \, d\Omega
\end{aligned}$$

Then, finally the weak problem is formulated as²:

Find $\mathbf{v} = (v_1, v_2) \in H_0^1(\Omega) \times H_0^1(\Omega)$ and $p \in L^2(\Omega)$ such as:

$$\begin{cases} ((\mathbf{v} \cdot \nabla) \mathbf{v}, \mathbf{u}) - \nu(\nabla \cdot \mathbf{v}, \nabla \cdot \mathbf{u}) - (p, \nabla \cdot \mathbf{u}) = 0 \\ (\nabla \cdot \mathbf{v}, q) - \epsilon(p, q) = 0 \end{cases}$$

$\forall \mathbf{u} = (u_1, u_2) \in H_0^1(\Omega) \times H_0^1(\Omega)$ and $\forall q \in L^2(\Omega)$.

Discretization

The discretization of the weak problem is formulated as follows:

Find $\mathbf{v}_h = (v_{1,h}, v_{2,h}) \in V_{h,k} \times V_{h,k}$, where k is the degree of the polynomial, and $p_h \in V_{h,k-1}$, such as:

$$\begin{cases} ((\mathbf{v}_h \cdot \nabla) \mathbf{v}_h, \mathbf{u}_h) - \nu(\nabla \cdot \mathbf{v}_h, \nabla \cdot \mathbf{u}_h) - (p_h, \nabla \cdot \mathbf{u}_h) = 0 \\ (\nabla \cdot \mathbf{v}_h, q_h) = 0 \end{cases}$$

$\forall \mathbf{u}_h \in V_{h,k} \times V_{h,k}$ and $\forall q_h \in V_{h,k-1}$. Because it is a non linear problem for v_h and p_h , an iterative method to solve the problem is required. Consequently, the Stokes equation will be used as a first approach (seed), then the solution obtained is employed as the initial solution for the larger Navier-Stokes expression. Hence:

Find $\hat{\mathbf{v}}_h \in V_{h,2} \times V_{h,2}$ and $\hat{p}_h \in V_{h,1}$, such as:

$$\begin{cases} \nu(\nabla \hat{\mathbf{v}}_h, \nabla \mathbf{u}_h) - (\hat{p}_h, \nabla \cdot \mathbf{u}_h) = 0 \\ -(q_h, \nabla \cdot \hat{\mathbf{v}}_h) - \epsilon(\hat{p}_h, q_h) = 0 \end{cases}$$

$\forall \mathbf{u}_h \in V_{h,2} \times V_{h,2}$ and $\forall q_h \in V_{h,1}$. Then, the solution obtained, $\hat{\mathbf{v}}_h$, is replaced in the Navier-Stokes equation, $\mathbf{v}_h^{(0)} = \hat{\mathbf{v}}_h$, and the iterative process is performed:

$$\begin{cases} ((\mathbf{v}_h^{(i)} \cdot \nabla) \mathbf{v}_h^{(i+1)}, \mathbf{u}_h) + \nu(\nabla \cdot \mathbf{v}_h^{(i+1)}, \nabla \cdot \mathbf{u}_h) - (p_h^{(i+1)}, \nabla \cdot \mathbf{u}_h) = 0 \\ (\nabla \cdot \mathbf{v}_h^{(i+1)}, q_h) = 0, \quad i = 0, \dots, N \end{cases}$$

²To get unique pressure, a perturbation term ($\epsilon \ll 1$ is added)

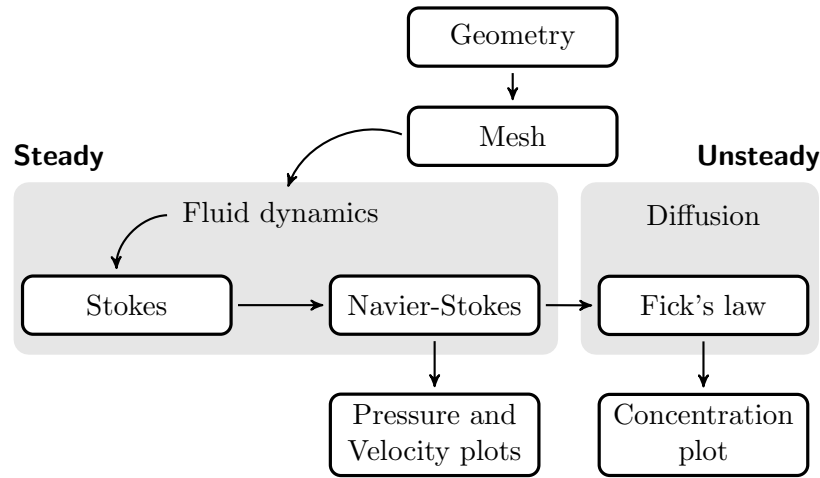


Figure 4.5: Flow chart of the operations performed in FreeFEM++.

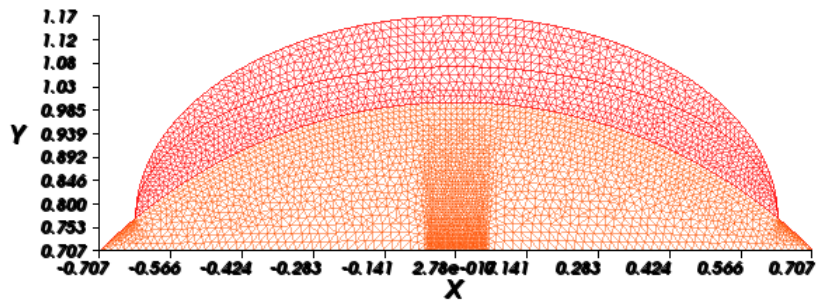


Figure 4.6: 7721 elements, 4021 vertices

4.4 Numerical results and analysis

Two cases are studied in this project. The first one is a healthy eye with an intraocular pressure of 17 mmHg. The input parameter is $0,2 \text{ mm s}^{-1}$ and the output is $0,1 \text{ mm s}^{-1}$. The second one is an eye with glaucoma and in this case the input and output parameters are changed in order to obtain a higher pressure. With an input of $0,3 \text{ mm s}^{-1}$ and an output of $0,1 \text{ mm s}^{-1}$ the intraocular pressure becomes 51 mmHg which is a severe case of glaucoma.

4.4.1 Meshing

The meshing of the domain shown in Fig. 4.2 is presented in Fig. 4.6 and Fig. 4.7. The former represents a coarser mesh composed of 7721 elements, whereas the latter comprises 17675 elements, being a finer mesh. In both of the meshes the separation between the anterior chamber (orange) and, contact lens and cornea (red), can be observed. Finer local meshing is displayed at the input of the aqueous humor as well as the outputs of the flow (Schlemm's canals).

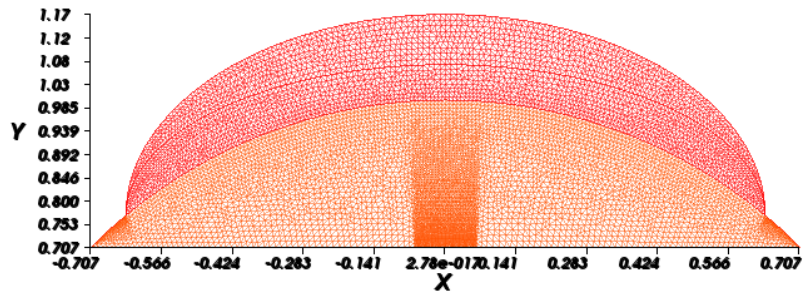
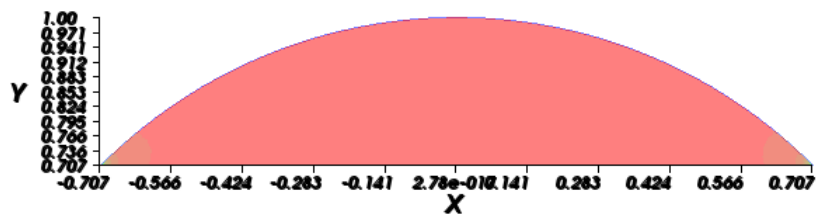


Figure 4.7: 17 675 elements, 9078 vertices

Figure 4.8: Pressure isolines in the anterior chamber. Healthy eye, $p = 17$ mmHg.

4.4.2 Pressure field

Fig. 4.8 shows the pressure distribution in the anterior chamber. The pressure is almost constant everywhere, except in the trabecular mesh where it is a bit lower due to the fluid output. This is the plot of the healthy eye, but the distribution of pressure is the same in the eye with glaucoma. However, the average value of the pressure in the eye with glaucoma is considerably higher ($p = 51$ mmHg).

4.4.3 Velocity field

The vector fields of the velocity for the healthy eye and the eye with glaucoma are shown in Fig. 4.9 and Fig. 4.10 respectively. It is clear from the plots that the input velocity for the eye with glaucoma is higher than the input velocity for the healthy eye. The color scheme is relative, so the output velocities are the same even though it looks like the output velocity through the trabecular mesh is lower for the eye with glaucoma. The magnitudes of the velocity in the simulation are coherent with the results obtained in [2].

4.4.4 Concentration field

In Fig. 4.11 the diffusion process is shown. In the beginning all the drug is concentrated in the contact lens, but as time goes by it moves towards the trabecular mesh. In this case the diffusion coefficients are high and that is why the process is so fast. In reality the diffusion coefficients would be lower, which makes the process slower.

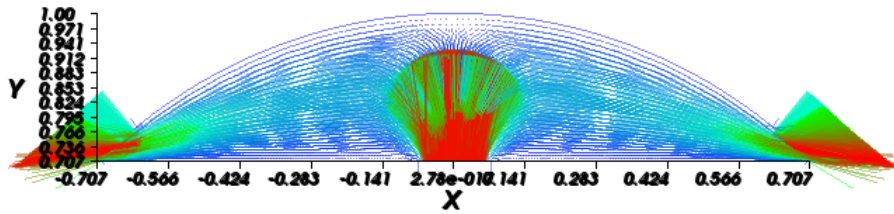


Figure 4.9: 17 mmHg: input = $0,2 \text{ mm s}^{-1}$, output = $0,1 \text{ mm s}^{-1}$

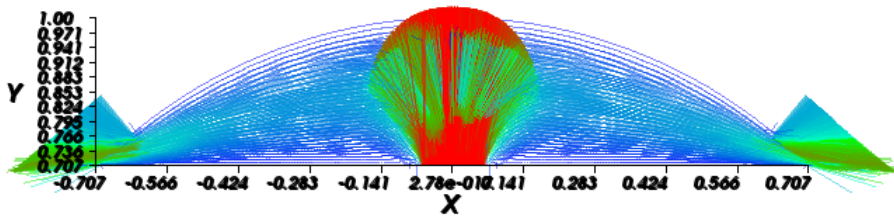


Figure 4.10: 51 mmHg: input = $0,3 \text{ mm s}^{-1}$, output = $0,1 \text{ mm s}^{-1}$

4.5 Conclusions and outlook

Our model is a very simplified one, and there is a lot that can be done to improve it. The main improvement would be to take the therapeutic effect into consideration. The goal is to treat the disease glaucoma by getting the drug to the trabecular mesh so that the mesh opens up and more fluid can leave the anterior chamber and the intraocular pressure decreases. In order to see this happening we would need to establish a connection between the concentration of the drug and the output through the trabecular mesh. Then we could couple our two problems, the fluid dynamics and the diffusion, and we would hopefully see that the drug works.

A further enhancement is taking into account that the flow in the anterior chamber is caused by thermal processes, as stated in [2] and [4]. That is, a temperature difference across the chamber is modelled, with a cooler anterior surface (the cornea) and a warmer posterior surface (the iris).

Other improvements would be to look at the real dimensions of the eye, consider the real properties of the aqueous humor (instead of treating the fluid as water), take more eye components into account (e.g. iris separation between anterior and posterior chamber) and include the bound and entrapped drug models discussed in the diffusion section.

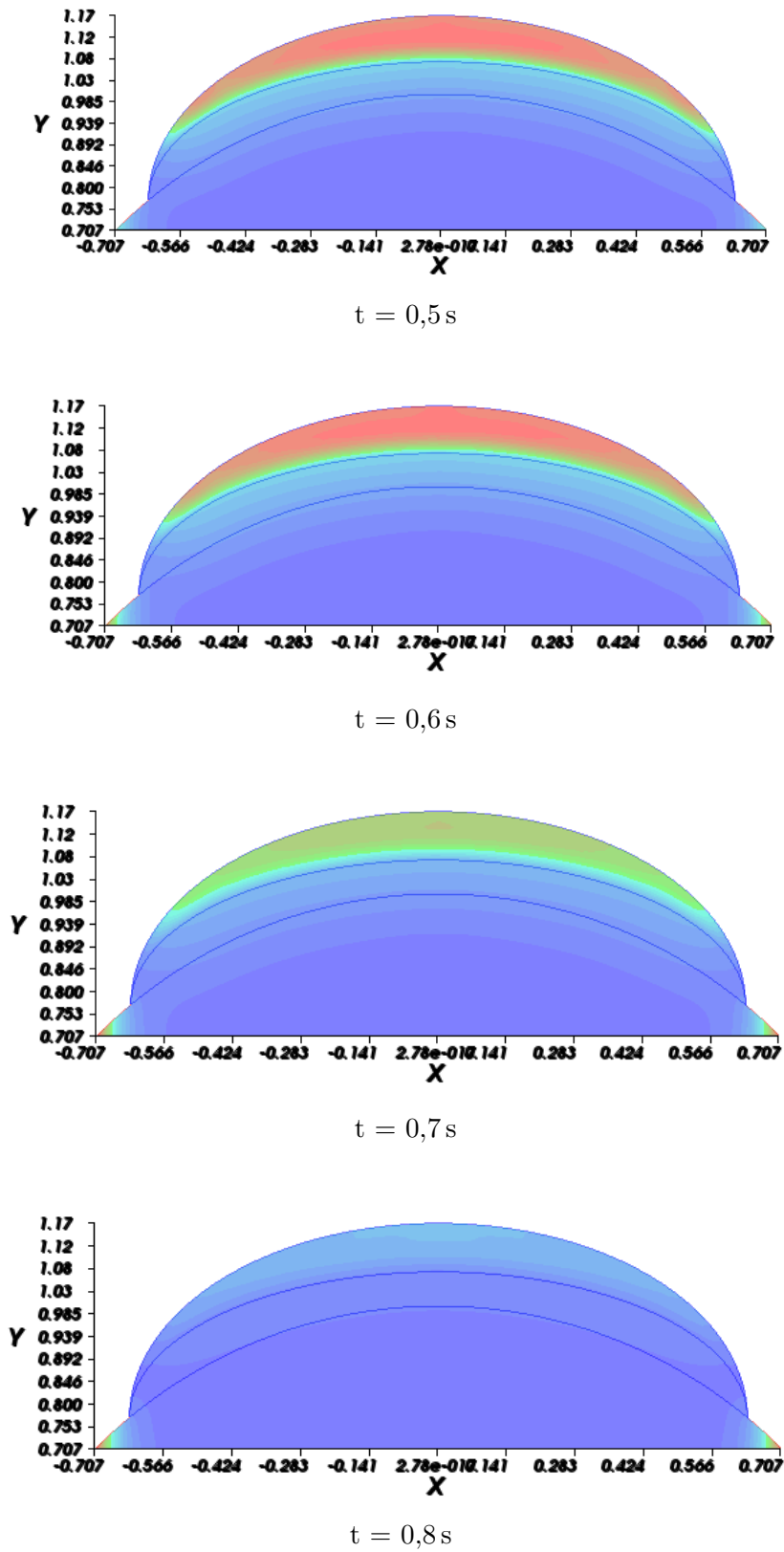


Figure 4.11: Evolution of the drug concentration for different time steps

Bibliography

- [1] Enric Mas-Aixala, Joan Gispets, Núria Lupón, Genís Cardona, *The variability of corneal and anterior segment parameters in keratoconus*, Contact Lens and Anterior Eye (2016).
- [2] Kor L. Tiang, Ean H. Ooi, *Effects of aqueous humor hydrodynamics on human eye heat transfer under external heat sources*, Medical Engineering and Physics 38 (2016) 776–784.
- [3] W. Daniel Stamer, Sietse T. Braakman, Enhua H. Zhou, C. Ross Ethier, Jeffrey J. Fredberg, Darryl R. Overby, Mark Johnson, *Biomechanics of Schlemm’s canal endothelium and intraocular pressure reduction*, Progress in Retinal and Eye Research 44 (2015) 86–98.
- [4] Ram Avtar, Rashmi Srivastava, *Modelling the flow of aqueous humor in anterior chamber of the eye*, Applied Mathematics and Computation 181 (2006) 1336–1348.
- [5] Samuel Gause, Kuan-Hui Hsu, Chancellor Shafor, Phillip Dixon, Kristin Conrad Powell, Anuj Chauhan, *Mechanistic modeling of ophthalmic drug delivery to the anterior chamber by eye drops and contact lenses*, Advances in Colloid and Interface Science 233 (2016) 139–154.